

<https://doi.org/10.1038/s41545-025-00539-2>

# Building-integrated solar water disinfection system for reliable year-round drinking water safety

Check for updates

Mandi Pretorius<sup>1,7</sup> ✉, Inhyeong Jeon<sup>2,3,7</sup> ✉, Mónica María Martínez-Fausto<sup>4</sup>, Nick Novelli<sup>1</sup>, Jorge Luis Galindo Arevalo<sup>4</sup>, Eric Ryberg<sup>5</sup>, Melanie M. Derby<sup>6</sup>, Jae-Hong Kim<sup>2</sup> & Anna Dyson<sup>1</sup>

Waterborne pathogens pose a major threat to global water safety. Solar energy could provide a critical opportunity for households without reliable access to safe water; however, many solar-driven household water treatment systems (HWTS) fail to provide adequate year-round quantities of clean drinking water, as they often cannot remove viruses during low-sun periods, exposing users to waterborne diseases. We demonstrate the disinfection capacity of a novel concentrating solar water-energy management system for building envelopes that integrates on-site water collection with phyto-derived photosensitization, solar water disinfection (SODIS), and solar pasteurization (SOPAS) within a roofing system suitable for a range of housing types. By combining outdoor testing in field settings with computational modeling, we demonstrate the water treatment capacity as a function of the year-round variations in solar resources available in different climates: Cape Town, South Africa; Sololá, Guatemala; and Phoenix, AZ, USA. Modeled annual performance across each site indicates that the approach could treat more than 70 L/m<sup>2</sup> per day of potable water, guaranteeing the United Nations (UN) minimum of 15 L per person per day, year-round. The integrated systemic approach reduces viral treatment times by up to two orders of magnitude compared to conventional SODIS, thereby achieving adequate daily water production rates that meet household needs, even in low solar periods. The building-integrated solar system combines water heating and disinfection, supplying up to 94% of domestic hot water demand, thereby reducing household energy costs and resource insecurity.

The World Health Organization (WHO) has warned that fecal contamination of drinking water poses the greatest threat to water safety, with up to 1.7 billion people relying on contaminated water globally in 2022<sup>1</sup>. Unsafe drinking water is associated with increased rates of diarrhea, malnutrition, and infections such as dysentery, cholera, hepatitis A, typhoid, and polio, and an estimated 446,000 annual diarrheal deaths among children younger than five years, accounting for 9% of yearly deaths in this age group<sup>2,3</sup>. Furthermore, an estimated 3 billion people will live in informal housing without access to basic services by 2050<sup>4</sup>.

Household Water Treatment Systems (HWTS) are crucial to providing safe drinking water and mitigating the economic and health impacts of waterborne disease, especially where the infrastructure for

drought resilience and/or centralized municipal water treatment is insufficient. HWTS are used by approximately one-third of populations within regions across Latin America, the Caribbean, Africa, the Eastern Mediterranean, Central and East Europe, and Southeast Asia<sup>5</sup>, with increasing public and private efforts to expand their accessibility. In other contexts, such as the United States, HWTS use has risen due to growing mistrust of domestic water safety and municipal infrastructure<sup>6–8</sup>. Considering that by 2050, a third of the global population of 9.7 billion will live in informal housing without access to services<sup>4</sup>, the development of affordable and effective HWTS must prioritize suitability for low-income or disadvantaged households, who are most vulnerable to inadequate water supply or resource insecurity.

<sup>1</sup>Yale Center for Ecosystems + Architecture (CEA), School of Architecture, Yale University, New Haven, CT, USA. <sup>2</sup>Department of Chemical and Environmental Engineering, School of Engineering and Applied Science, Yale University, New Haven, CT, USA. <sup>3</sup>School of Health and Environmental Science, Korea University, Seoul, Republic of Korea. <sup>4</sup>Centro de Estudios Atitlán, Instituto de Investigaciones, Universidad del Valle de Guatemala, Guatemala, Guatemala. <sup>5</sup>Department of Allied Health Sciences, University of Connecticut, Storrs, CT, USA. <sup>6</sup>Alan Levin Department of Mechanical and Nuclear Engineering, Kansas State University, Manhattan, KS, USA. <sup>7</sup>These authors contributed equally: Mandi Pretorius, Inhyeong Jeon. ✉e-mail: [mandi.pretorius@yale.edu](mailto:mandi.pretorius@yale.edu); [inhyeong@korea.ac.kr](mailto:inhyeong@korea.ac.kr)

Precedent HWTS treat water through removal (e.g., filtration, absorption, sedimentation) or inactivation, such as solar disinfection. Each technology has different disinfection capacities, operational energy consumption, input materials, or user oversight (Table S1). To develop distributed water treatment approaches suitable for a wide range of dwelling types, several limitations of incumbent HWTS are considered here: the effectiveness of treatment, the security of system input resources, and the scalability of the system. Firstly, many low-cost HWTS approaches typically use a single treatment mechanism with variable effectiveness against specific pathogens, presenting limited broad-spectrum protection (Table S1). For instance, ceramic filtration, while capable of removing bacteria, fails to remove smaller pathogens, such as viruses, which can pass through the filter systems<sup>9</sup>. HWTS performance in realistic use-settings drops substantially compared with disinfection capacity reported within controlled testing, with most HWTS failing to meet WHO standards for effective point-of-use (POU) systems (Table S1). Furthermore, many input materials and their disinfection by-products (DBPs) have been linked to detrimental human health effects with long-term use<sup>10</sup>. Field applications of available HWTS in rural or developing contexts typically focus on adopting a single technique to reduce user costs and complexity, albeit at the cost of broad-spectrum performance<sup>11</sup>. By contrast, most commercial systems for installation in homes or offices adopt multi-barrier systems combining several technologies in a flow-through system to increase water safety. However, these precedent systems are typically too costly and unsuitable for widespread adoption in low-income or informal households that often struggle with limited resource access daily<sup>12</sup>.

Second, the input material and energy dependence of many HWTS increases the vulnerability of low-income, resource-constrained households. Boiling drinking water is the most predominant HWTS globally, used by nearly 1.1 billion people in 67 countries<sup>7</sup>. It is an effective POU treatment that leverages the visual indication of boiling as a safeguard informing users the water is safe to drink<sup>13,14</sup>. However, water boiling demands more energy than other treatment approaches, requiring 1 kg of firewood per liter of water or 0.1 kWh/L energy for electric boiling<sup>15</sup>. Therefore, for the UN recommendation of 15 L potable water per person, this energy input requirement is prohibitive for many low-income households who may rely on daily collection of firewood or organic fuel sources to boil water and supply other energy needs<sup>16,17</sup>, placing a higher cost burden and risk that they cannot secure enough fuel each day.

In contrast, the use of available solar energy reduces the energy burden with solar disinfection (SODIS), solar pasteurization (SOPAS), solar distillation, as well as the use of photocatalysts and photosensitizers. With solar pasteurization (SOPAS), the input energy required to attain a recommended 65 °C water temperature for 6 min is less than half that of boiling<sup>18</sup>. The time-temperature safety zone for effective microbiological inactivation by SOPAS is a well-established means of achieving treatment, even with lower temperatures<sup>19,20</sup>, inactivating bacteria through heat-induced cellular degradation at temperatures > 55 °C and inactivating viruses by denaturing viral proteins at temperatures > 75 °C<sup>19</sup>. Although SOPAS disinfection occurs in minutes at target temperatures and has a far higher disinfection capacity (L/m<sup>2</sup>/day) than other solar disinfection technologies<sup>21</sup>, the capacity to reach SOPAS temperatures within a solar thermal collector depends on solar intensity and ambient conditions. For instance, over colder months, the hot water output of solar thermal collectors, such as flat plate collectors, could drop to 30% that of peak solar months<sup>22</sup>. As a result, SOPAS systems require longer residence times over low-sun or cooler periods and are more susceptible to hourly solar intensity changes that could compromise water safety if temperatures are not maintained during treatment. Therefore, SOPAS is typically nonviable under cloud cover, requires longer treatment times in partially cloudy conditions, and, thus, cannot guarantee adequate volumes of safe water throughout the year for some climates if used in isolation.

Conventional SODIS faces similar challenges with solar availability. As recommended by the WHO, households practice

conventional SODIS by placing clear plastic water bottles in the sun for recommended periods<sup>23,24</sup>. SODIS depends on UV-B solar energy to induce DNA damage or UV-A generation of ROS to inactivate microorganisms through accumulated cellular damage as a function of solar dosage. However, as the total UV component makes up less than 5% of the terrestrial solar energy spectrum, conventional SODIS could require over 30 h of solar exposure to inactivate viruses to the EPA minimum 99.99% water disinfection standards<sup>25,26</sup>. As a result, to provide effective disinfection, conventional SODIS requires long treatment times, which limit daily water production in sufficient quantities and timely access to safe drinking water on demand. Lacking a visual indication of when the water is ready to drink, as well as a reliable means of ensuring effective treatment in non-ideal solar conditions, these factors contribute to mistrust and limited SODIS adoption among less than 1% of global HWTS users.

Third, there is a lack of investment in making renewable distributed water treatment approaches suitable for bolstering drought resilience in urban environments, where the majority of the global population is estimated to live by 2050<sup>27</sup>. Many affordable water treatment techniques are viewed as haphazard, temporary solutions with limited effectiveness due to a lack of formalization<sup>12,28</sup>. Numerous studies have attempted to scale various solar treatment techniques in formalized systems to increase performance stability and user adoption<sup>12,28,29</sup>. For instance, there is an abundance of literature on parabolic and compound parabolic (CPC) solar concentrating collectors for water treatment<sup>30–33</sup>, several of which have been deployed in the field at household to community-scale systems<sup>12,28,34</sup>. However, these precedent systems are commonly standalone devices that require manual operation and would occupy a large footprint on a user's property, potentially competing with other daily household activities and straining households' time and resources.

Towards achieving the preceding criteria—*efficacy, resource security, and scalability relative to households' needs*—in this study, we assess the annual disinfection capacity of a novel flow-through, building-integrated water treatment system<sup>35</sup>, an embodiment of the Solar Enclosure for Water Reuse (SEWR) framework<sup>36</sup>. With SEWR, we demonstrate opportunities in building-integrated HWTS that utilize renewable, non-toxic resources to ensure adequate disinfection year-round, while simultaneously fulfilling other building functions, thereby reducing household costs and risks.

Investigating year-round performance, the study critically evaluates the complementary benefit of multiple treatment strategies within the SEWR system by combining outdoor testing with computational modeling to thoroughly compare the disinfection capacity of the different system treatment mechanisms under various geographic locations and times. The experimental objectives include (1) evaluating the field performance of the system concept in realistic use settings, (2) using the field performance data in computational modeling of the annual water treatment capacity of the multi-mechanism system in several climate locations, and (3) modeling the potential increase in daily water production if we integrate a prefiltration stage into the system, and (4) the production of domestic hot water and estimated reduction in household energy demand.

## Results

### Field testing: bacterial disinfection capacity by SOPAS and SODIS factors

The system achieved high levels of bacterial inactivation under SODIS and SOPAS operation. We used a batch heating protocol to collect samples at set temperature points that correspond with established SOPAS performance parameters to evaluate the system's upper limits in disinfection capacity within a building-integrated flow-through system. Challenged at elevated *E. coli* concentrations to evaluate maximum performance, the system demonstrated a 99.99999% log reduction of *E. coli* (7.9 LRV) to below detectable limits (1 CFU/mL) at mean water temperatures of 75 °C and 1100 W/m<sup>2</sup> irradiance (Figs. 1a and S2). These results correlate with established SOPAS time-temperature

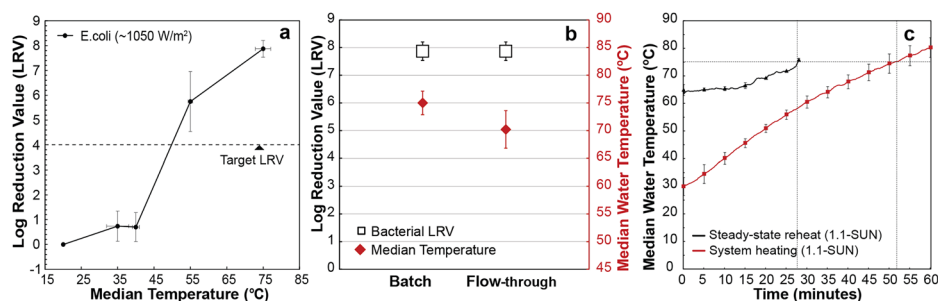


**Fig. 1** | a–c Outdoor field testing in Sololá, Guatemala. **a** *E. coli* LRV by median water temperature: at >55 °C, the system produced over 5-log *E. coli* inactivation and 7.9-log at 75 °C with batch heating ( $n = 3$ ;  $n =$  median water temperature under 1050 W/m<sup>2</sup>). **b** *E. coli* LRV by flow control: Modulating residence time in either batch or flow-through configurations, the system achieved >7.8 bacterial LRV at

between 70–75 °C median water temperatures with both configurations (1100 W/m<sup>2</sup>). **c** From ambient, the system required 50–55 min to reach steady-state SOPAS water temperatures (1100 W/m<sup>2</sup>), thereafter attaining SOPAS temperatures within 25–30 min reheating cycles at steady-state. Error bars show standard deviation ( $n = 3$ ;  $n =$  median water temperature under 1.1-SUN irradiation).

relationships whereby 6-log inactivation occurs at >70 °C outflow temperatures<sup>19</sup>. With samples collected at lower effluent temperatures (mean 55 °C, ~1000 W/m<sup>2</sup>), we observed an average 5.8 LRV, corroborating literature review findings that SOPAS inactivation can occur at temperatures above 55 °C<sup>19</sup>.

Depending on solar availability, the system can modulate solar dosage through flow rate to adjust the residence time and degree of water heating to guarantee water safety over periods of intermittent sunshine. Herein, continuous flow systems are advantageous and desirable if we are to achieve large-scale and/or viable solar water treatment systems that produce adequate volumes of treated water<sup>28,37</sup>. Therefore, following sample collection at increased water temperatures in the batch testing condition, we evaluated the disinfection capacity of the system in a flow-through condition (10 mL/min) that corresponds with continuous flow studies reported in the literature<sup>29,38,39</sup>. Herein, the effluent temperatures depend on the solar availability across the period of solar exposure at the set flow rate. Under full sun conditions, the flow-through condition produced a 7.9-log reduction (1050 W/m<sup>2</sup>) at a mean 78 °C effluent temperature, matching the batch testing performance (Fig. 1b). Considering the importance of stable system performance to guarantee water safety, these results validate using mean water temperature within the system reactor as a performance indicator in batch and flow-through configurations.

To simulate daily water treatment capacity under SOPAS operation, we assessed the water production rate over the peak solar period as a function of the time required to reach the target effluent temperature. Initial heating of the system from cool overnight temperatures and under 1100 W/m<sup>2</sup> irradiance took on average 50–55 min to reach 75 °C median water temperatures (20 °C ambient temp, 10:00 am start time) (Fig. 1c). These results suggest that the system would complete the first batch treatment cycle by mid-morning, after which the system cycles through consecutive treatment batches for the remainder of the daily solar period. Once at steady-state, the system provided stable heating rates, achieving mean 75 °C water temperatures within an average of 28 min between treatment batches (Fig. 1c).

The system achieved adequate water treatment in low sun conditions with intermittent irradiance levels, albeit at reduced overall inactivation rates (Fig. S3). Samples at a median temperature of 73 °C produced a 5.3 LRV under an average 575 W/m<sup>2</sup> solar intensity, exceeding minimum treatment standards<sup>26</sup>. Under initial cloudy conditions at ~300 W/m<sup>2</sup> irradiance, the heating rate decreased 8-fold relative to full sun heating rates. From 21 °C feed temp, the median water temperature increased to 35 °C in 103 min (18 °C ambient, 55% RH), by comparison to 12 min under 1000 W/m<sup>2</sup> (21 °C ambient, 59% RH) (Fig. S3). With intermittent sunshine and fast-moving partial cloud cover (~610 W/m<sup>2</sup>), the system reached the minimum median temperature of 50 °C in 2.6× the time observed with clear sky testing (Fig. S3).

### Field testing: viral inactivation by SOPAS, SODIS, and photosensitization factors

The system's viral inactivation capacity is a function of SODIS, SOPAS, and photosensitization. As the disinfection capacity of photosensitization is less dependent on environmental and geospatial factors than with SOPAS, it is the dominant virus removal technology in the combined system approach. Field setting constraints prohibited physical testing with virus proxies. Based on the substantial characterization of photosensitization kinetics, the field testing of the photosensitizer photon-absorption-driven decay (i.e., photobleaching) provided an estimate for the system's viral LRV and treatment times.

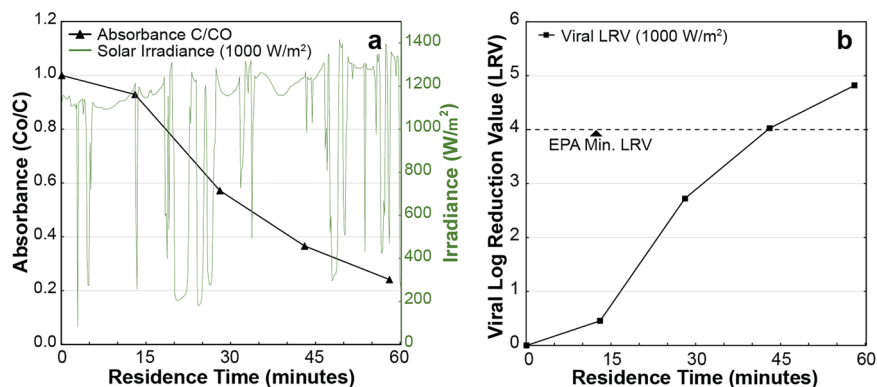
Outdoor testing was conducted with the *Case 4-Combined* reactor configuration used in performance modeling, combining the treatment technologies. The rate of photobleaching color loss in field settings (72.35% decay, ~1025 W/m<sup>2</sup> irradiation) suggests that the *Case 4* configuration could produce a ~4 LRV over 45 min, showing that the system could provide comprehensive virus inactivation that meets the EPA minimum in less than an hour (Fig. 2). The results suggest that the water treatment rate for SOPAS and photosensitization is commensurate under optimal solar conditions (Avg: 30 min, >4 LRV). During cloudy or colder environmental conditions, when SOPAS heating rates decrease to below what is required for thermotolerant viruses (>75 °C), the comparatively shorter residence time of the photosensitization mechanism will likely dominate as the primary viral disinfection mechanism, as illustrated by the modeled performance in the following section.

Based on the modeled extrapolation of measured inactivation rates incorporated into the concentrating solar system for the *Case 4-Combined* configuration, the photosensitization mechanism could provide the EPA minimum 4-log inactivation within 104 min under ~300 W/m<sup>2</sup> or 33 min in ~600 W/m<sup>2</sup> irradiation. Furthermore, to achieve sufficient bacterial inactivation (4-log) under the same irradiation levels, modeled estimates suggest that SODIS would be affected within 123 and 62 minutes, respectively (*Case 4-Combined*). Therefore, in the worst-case scenario with limited sunshine averaging 300 W/m<sup>2</sup>, the system could ensure adequate water disinfection within 2-h, vastly increasing drinking water access relative to conventional SODIS that requires greater than a day in these low-sun solar conditions<sup>40</sup>. The system's performance in non-ideal solar periods demonstrates the value of the synergistic incorporation of several solar-driven treatment mechanisms in overcoming limited solar availability. Nevertheless, future studies should include direct viral inactivation experiments under field-relevant conditions to further validate the predictive accuracy and robustness of the SEWR system's disinfection performance.

### Modeled performance: SEWR annual disinfection capacity without prefiltration

The experimental results suggest that the SEWR system can effectively treat waterborne pathogens under varying solar intensities. To further validate

**Fig. 2 | Photosensitization by residence time.** **a** The photo decay curve linearly correlates with photosensitization of virucidal ROS under solar irradiation. **b** Outdoor testing under full sun produced a 72.35% decay in 45 min, an indirect estimation of a ~4 LRV in MS2 (Proxy).



the disinfection capacity, we use computational modeling to assess the impact of solar availability and climate on system performance and its ability to meet annual daily water needs. We analyzed hourly and daily variations in disinfection capacity across systems in three modeled cities: Sololá, Phoenix, and Cape Town (Figs. 3a, b and S5). Cape Town and Sololá represent highly seasonal climates with wet and dry periods that typify the challenges in solar-driven water management. Herein, numerous subtropical to temperate climates face limited solar availability during heavy rains when water contamination levels often peak or struggle with prolonged periods of drought that demand safe water storage. In contrast, Phoenix's semi-arid desert climate offers more consistent year-round temperatures and insolation, illustrating system performance in optimal conditions. The evaluation highlights how disinfection capacity varies by site, depending on climate, geography, and solar availability, and quantifies the contributions from each treatment mechanism to illustrate the value of the synergistic treatment approach in SEWR.

In all modeled cities, the synergistic system design combining the several treatment mechanisms (*Case 4-Combined*) consistently exhibited the highest disinfection capacity compared to each mechanism in isolation (*Case 1, 2, and 3*). As illustrated in Fig. 3c, depending on the time of day, *Case 4*'s capacity was primarily driven by one of the several disinfection mechanisms that are incorporated into the system (Text S6). When we examined what mechanism predominantly determines the overall hourly water production (Fig. 3c and Text S6), photosensitization played a crucial role in disinfection in the fourth case when SOPAS was less effective, thereby extending the operational time and daily water production of the SEWR system. Virus inactivation through either SOPAS or photosensitization dictates the overall capacity between 10:00 am and 2:00 pm, while bacteria inactivation via SODIS is crucial for the remaining hours. This highlights that the multi-mechanism strategy could further enhance the resilience of the water treatment system by diminishing reliance on a single disinfection mechanism.

Second to the combined system (*Case 4*) with an average median treatment capacity of  $>70 \text{ L/m}^2/\text{day}$ , the *Case-3 Photosensitization* configuration can produce an average of median values of  $>58 \text{ L/m}^2/\text{day}$  in all three modeled deployment cities (Fig. 3a). Pathogen inactivation occurs in this configuration through photosensitization for viruses and SODIS for bacteria. Therefore, the overall disinfection capacity is limited by the longer residence times required for SODIS to inactivate bacteria compared to the shorter time needed for virus inactivation through photosensitization.

In contrast, the median water production in the *Case-2 SOPAS + SODIS* configuration with a  $1 \text{ m}^2$  system exceeds  $60 \text{ L/m}^2/\text{day}$  in Phoenix but averaged to  $41 \text{ L/m}^2/\text{day}$  in Cape Town and Sololá which have more pronounced wet seasons and therefore less ideal conditions for SOPAS treatment alone. Additionally, the *Case 1-SODIS* configuration failed to produce more than  $7.4 \text{ L/m}^2/\text{day}$ , far below the minimum emergency drinking water requirements of at least  $15 \text{ L/day}$  (UN Sphere, 2018). As these results demonstrate, irrespective of the concentrating solar effect of the

collector design, the SODIS disinfection mechanism (*Case 1-SODIS*) is an ineffective treatment approach when used in isolation.

### Modeled performance: enhanced water production with prefiltration

Modeling shows that the SEWR system (*Cases 3 and 4*) can meet the minimum emergency drinking water demands of  $15 \text{ L}$  per person per day in all three climate locations, overcoming seasonal variations in solar availability or cloud cover that typically limit the performance of incumbent systems. This achieves the most basic requirement of HWTS systems: households have a viable means of treating their drinking water on-site and securing water safety year-round. Having shown this, we investigate how the SEWR approach could be modified to increase daily water production by incorporating a prefiltration stage. A key challenge for most HWTS is adequate virus removal. While many low-cost HWTS in LMICs effectively inactivate bacteria, they often fail to remove viruses in real-world settings (Table S1). Therefore, in modeling the annual performance of SEWR incorporated with a prefiltration stage, we show the added disinfection capacity possible if individual HWTS are incorporated in user-friendly and cost-effective multi-barrier approaches.

We compared the system's disinfection capacity in isolation with its modeled performance when installed in a multi-barrier configuration that includes prefiltration. By incorporating a prefiltration stage that removes bacteria, we observed that *Case 3-Photosensitization + SODIS* produced the highest disinfection capacity in all cities (Fig. 3a). *Case 4-Combined* showed a lower disinfection capacity than *Case 3-Photosensitization + SODIS* when a prefiltration stage is included. This is because *Case 4* incorporates a solar absorptive coating on the bottom half of the tube for SOPAS (Fig. 4), which significantly reduces irradiation for photosensitization, thereby reducing *Case 4*'s viral inactivation rate. These findings provide an example of performance trade-offs that must be considered on a site-by-site basis. A multi-barrier system with prefiltration and *Case 3* could provide higher volumes of treated water. The disinfection capacity of *Case 1-SODIS* and *2-SOPAS* was not affected by the addition of a prefiltration stage because viruses exhibit greater resistance to SODIS and SOPAS treatment than bacteria.

### Modeled performance: daily household potable water demand

Household water consumption patterns have seasonal and climatic variations. Regardless of seasonal changes in resource availability, the system must provide a guaranteed minimum capacity to treat at least  $15 \text{ L}$  per person per day<sup>41</sup> using 100% solar energy, with no more than 2–3 days of intermittency or reliance on bottled water. We assumed a 4-person household in each city (Sololá, Phoenix, and Cape Town) using a  $4 \text{ m}^2$  SEWR system and evaluated the system's ability to provide  $180 \text{ L}$  of water, corresponding to the minimum drinking water demand of one household for three days, for any three consecutive days (Table 1). Based on these assumptions, we found that the third and fourth cases (*3-Photosensitization* and *4-Combined*) could successfully satisfy the

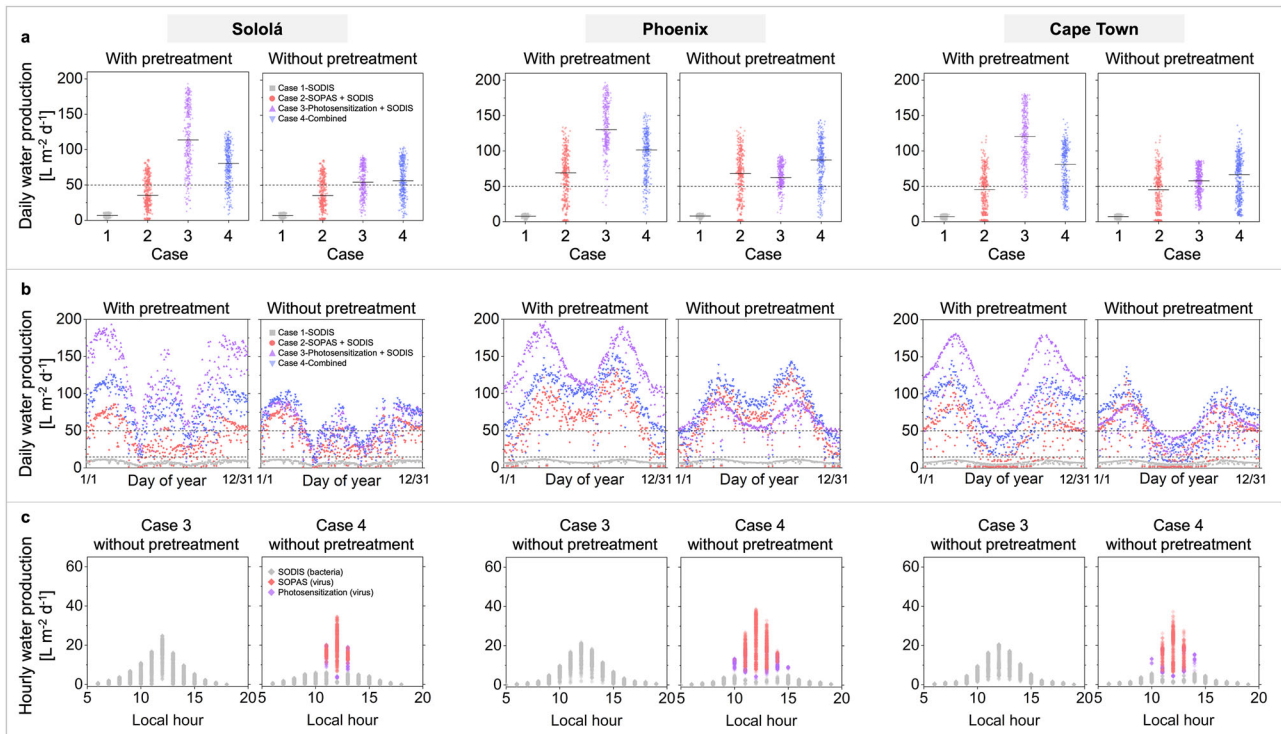


**Fig. 3 | Daily and hourly disinfection capacity in three different cities (i.e., Sololá, Phoenix, and Cape Town) based on computation modeling.** **a** Distribution of daily disinfection capacity in four different cases, both with and without prefiltration. Each dot, represented in various colors, corresponds to the daily disinfection capacity for a specific case, calculated by summing the hourly disinfection capacities (Text S1–S5). The horizontal lines represent the median value for each case. The horizontal dotted line indicates the UN minimum water requirement per person for all potable uses (e.g., cleaning and hygiene) and adequate health, which is 50 L/d. **b** Distribution of daily disinfection capacity as a function of the day of year. The

upper horizontal dotted line, which is 50 L/d, indicates the UN minimum potable water requirement per person, while the bottom horizontal dotted line, which is 15 L/d, represents a minimum drinking water demand per person. **c** Hourly distribution of disinfection capacity over a year as a function of local time in Case 3 and Case 4 without pretreatment. Each dot represents the disinfection capacity on a specific day of the year, with colors indicating the dominant disinfection mechanism: bacteria inactivation by SODIS (gray), virus inactivation by SOPAS (red), or virus inactivation by photosensitization (purple).

**Fig. 4 | SEWR system configurations dependent upon application.** **A** Configurations in which the receiver is comprised of a clear quartz tube. **B** Configurations in which the receiver is modified with a solar thermal coating, that is applied to the reflector-facing side of the receiver.

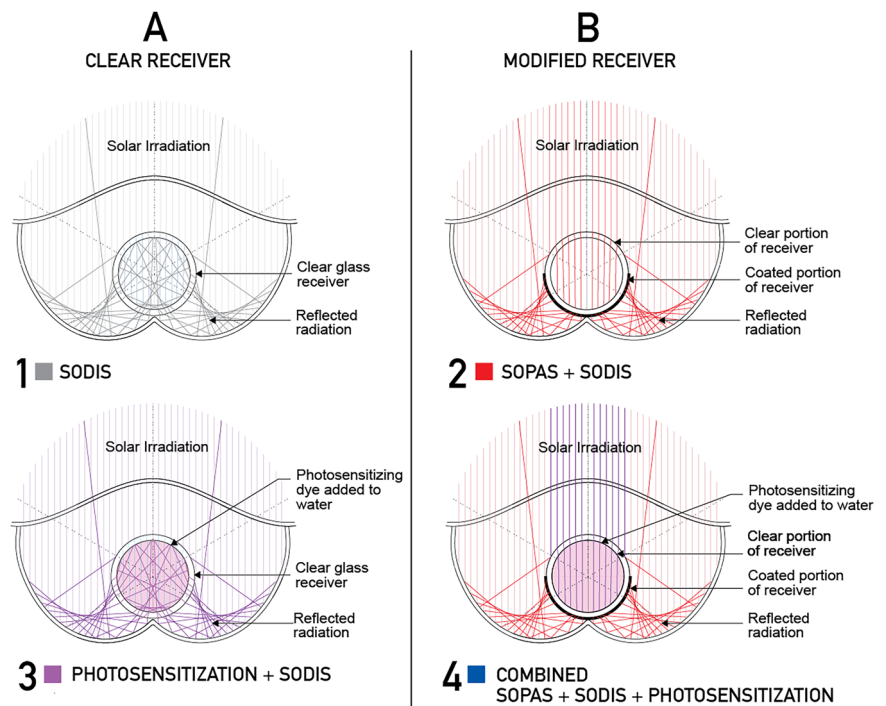


**Table 1 | Daily household potable water and hot water production using the SEWR system**

City	Pretreatment	Scenario	Daily water production (L day <sup>-1</sup> ) <sup>a</sup>			# of days of failing to produce the minimum drinking water demand for 3 consecutive days	# of days of failing to produce the minimum demand for all potable water uses	# of days of failing to produce the minimum requirement of hot water (>60 °C)
			Minimum	Average	Maximum			
Sololá	Yes	1 SODIS	3.12	28.46	46.88	365	365	NA
		2 SOPAS	2.04	158.21	342.48	13	233	81
		3 Photosensitization	51.32	468.86	772.42	0	23	NA
		4 Combined	33.61	314.21	502.89	0	61	81
	No	1 SODIS	3.12	28.46	46.88	365	365	NA
		2 SOPAS	2.04	158.21	342.48	13	233	81
		3 Photosensitization	24.6	224.7	370.3	0	147	NA
		4 Combined	16.11	234.75	417.83	5	140	44
Phoenix	Yes	1 SODIS	5.73	32.36	47.78	365	365	NA
		2 SOPAS	2.7	260.43	534.13	23	110	42
		3 Photosensitization	94.47	533.13	787.25	0	9	NA
		4 Combined	44.51	378.35	615.78	0	32	23
	No	1 SODIS	5.73	32.36	47.78	365	365	NA
		2 SOPAS	2.7	260.43	534.13	23	110	42
		3 Photosensitization	45.28	255.56	377.36	0	58	NA
		4 Combined	21.34	330.58	573.46	0	74	21
Cape Town	Yes	1 SODIS	8.29	28.51	43.9	365	365	NA
		2 SOPAS	4.07	168.79	484.14	68	191	115
		3 Photosensitization	136.6	469.7	723.4	0	19	NA
		4 Combined	67.05	302.04	578.9	0	100	72
	No	1 SODIS	8.29	28.51	43.9	365	365	NA
		2 SOPAS	4.07	168.79	484.14	68	191	115
		3 Photosensitization	65.48	225.15	346.77	0	138	NA
		4 Combined	32.14	243.92	545.4	0	144	58

<sup>a</sup>Daily water production for a 4-person household using a 4 m<sup>2</sup> SEWR system.

minimum demand in every city year-round, even without prefiltration (Table 1), demonstrating the potential of the SEWR system as a viable and scalable approach that could respond to an immediate need for effective HWTS.

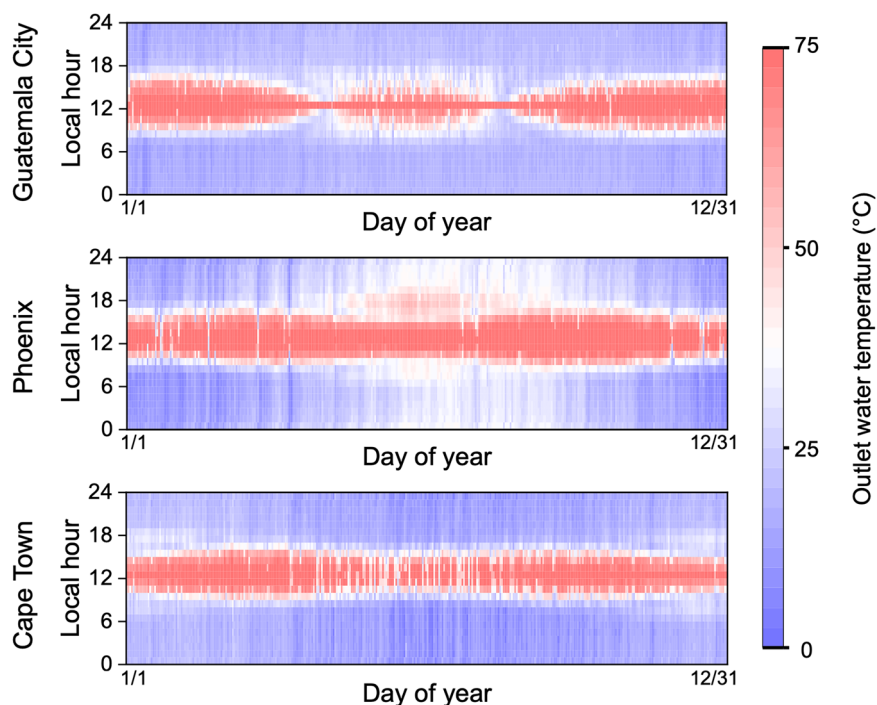
In addition to drinking purposes, potable water is required for other uses, such as cleaning and hygiene. The United Nations (UN) determined a 50 L minimum potable water demand per person, excluding non-potable demands that can be supplied with recycling and reuse<sup>42</sup>. We found that the third and fourth cases could not meet this requirement during the rainy seasons (May–September) in Sololá and Cape Town without pretreatment (Table 1 and Fig. 3b). This highlights the impact of climate on SEWR system performance, particularly in regions with long rainy seasons. However, implementing a prefiltration stage could still improve the daily water production in these regions (Table 1). In the third case (3-Photosensitization), days of failure to meet the 50 L water demand were significantly reduced, around seven times, resulting in less than 20 days of failure, even in Sololá and Cape Town. These findings demonstrate that the multi-barrier approach, using pretreatment, is highly recommended to achieve higher water production volumes during the rainy season in some regions. In contrast, in Phoenix, without a noticeable rainy season, both cases (3-Photosensitization and 4-Combined) could fully ensure the water demand for all portable uses except winter, specifically during December and January. The multi-barrier approach with prefiltration could further enhance the system efficiency, resulting in only 9 and 32 days of failure for the third and fourth cases, respectively. This suggests Phoenix, or

regions with similar climates, is an ideal application for the SEWR system to meet all potable water demands.

The modeled performance of the SEWR system demonstrates why a multi-barrier or multi-mechanism approach is essential to guaranteeing year-round water safety, which most single-mechanism HWTS fail to achieve. Due to the combined disinfection capacity of several treatment mechanisms, the SEWR system (*Case-4 Combined*, without pretreatment) has an estimated average annual daily water production of 59, 83, and 61 L/m<sup>2</sup>/d in Sololá, Phoenix, and Cape Town, respectively (Fig. 3a). If we include a prefiltration stage, the average daily SEWR disinfection capacity increases to 79, 95, and 76 L/m<sup>2</sup>/day for each of the latter field sites, respectively. The combined disinfection capacity of several treatment mechanisms could allow for peak treatment rates of 24 L/m<sup>2</sup>/h in Phoenix, 19 L/m<sup>2</sup>/h in Sololá, and 17.4 L/m<sup>2</sup>/h in Cape Town (Fig. S6).

Due to the enhanced disinfection through combining solar concentration with several treatment techniques, the SEWR system could inactivate bacteria and viruses at an average annual hourly rate of water treatment exceeding 5.03 L/h (Sololá: 5.34 L/hr; Phoenix: 7.02 L/h; Cape Town: 5.25 L/h) that could ensure households' adequate and timely access to drinking water. In addition, incorporating photosensitization and solar concentration vastly reduces the viral treatment time from up to 30 h with conventional SODIS to less than 6.3 min with Case-3 Photosensitization under peak solar (1000 W/m<sup>2</sup>). Doing so increases the potential for effective use of available solar by up to two orders of magnitude, especially during periods of intermittent sunshine when rapid treatment rates could allow for adequate water treatment in limited solar windows.

**Fig. 5 | Potential of the SEWR system (i.e., Case 4-Combined without pretreatment) for domestic hot water production in different cities.** The SEWR system can produce sufficient hot water (>60 °C), more than 80 L per household with 4 m<sup>2</sup> of the system, for over 90% of the year across all three cities.



### Modeled performance: domestic hot water

In addition to water disinfection, the SEWR system incorporating SOPAS can generate domestic hot water, reducing household energy costs (fuel, electricity) and vulnerability to a lack of energy sources. Across the field sites, water heating makes up 18% of domestic energy in Phoenix<sup>43</sup> and between 40–60% of Cape Town middle-income household budgets<sup>44</sup>. In Guatemala, 57% of a low-income household's energy consumption is based on firewood, while in middle-class households, over 28% of a household's electricity bill could be spent on powering in-line electric water heating<sup>45,46</sup>.

As a further reduction of the energy burden of domestic water heating, we demonstrate the system's capacity to meet year-round hot water demands. We assume the system must ensure that at least 40% of the minimum 50 L daily water demand per person is heated to DHW requirements<sup>47</sup>. We evaluated the outlet water temperature of the SEWR system integrating SOPAS in three countries. We calculated the daily hot water production at a temperature greater than 60 °C while achieving water disinfection. DHW for cooking and hygiene must retain a > 60 °C temperature to mitigate *Legionella* growth and contamination (32–35 °C, <45°)<sup>20,48,49</sup>. The minimum hot water demand was set at 80 L per household, and the number of days when the system failed to produce this amount was summarized in Table 1.

In all three cities, *Case 4-Combined* outperformed *Case 2-SOPAS + SODIS*. In *Case 2-Combined*, the SOPAS disinfection capacity (Fig. 5) depends upon the outlet water temperature exceeding 75 °C to ensure virus inactivation. This means that although the water temperature inside the reactor is higher than 60 °C, it is still insufficient to achieve water disinfection, thereby failing to meet the system's combined water treatment and heating objectives. In contrast, *Case 4-Combined* had more diverse treatment strategies, sometimes enabling water disinfection at a temperature lower than 75 °C or 65 °C for virus and bacteria pasteurization, respectively. Interestingly, *Case 4-Combined* without pretreatment had an even lower number of failures compared to that with the pretreatment. This is because, in some instances with pretreatment, virus inactivation via photosensitization is so effective that it accelerates the water flow, preventing the water from reaching the desired temperature of 60 °C. However, assuming a user-facing interface is

available in practical applications, the SEWR system user could slow the water outflow rate to ensure adequate water heating and disinfection. With this adjustment, *Case 4-Combined* with pretreatment would perform better regarding water heating than *Case 4-Combined* without pretreatment. This demonstrates another advantage of the SEWR system, as users have the flexibility to optimize operation by either maximizing water production or prioritizing water heating.

*Case 4-Combined* without pretreatment can produce the minimum hot water requirement throughout the year, except for one or two months during the rainy seasons or winter (Fig. 5). Without pretreatment, the best scenario for water heating (*Case 4-Combined*) produced sufficient hot water for 88% of the year in Sololá (321 days), 94% in Phoenix (344 days), and 84% of the year in Cape Town (307 days). Therefore, the building-integrated solar system could provide hot water for most of the year, substantially reducing household energy costs in water heating. Based on a water-conscious consumption of 200 L per household per day and a minimum 40% hot water component, estimates suggest that the relative water heating proportion of household energy bills could be reduced by 17% for Phoenix, 26% for Guatemala households, and up to 50% for Cape Town, potentially alleviating household energy burdens and dependence on grid energy.

### Discussion

To achieve *effective* water treatment, which considers household *resource security* and is *scalable* for use in housing, this study aims to address several limitations in developing effective on-site water treatment capacity based on renewable energy and material inputs. Enhancing the viability of solar-based disinfection systems, with SEWR, we demonstrate opportunities for incorporating HWTS as a building-integrated system that combines solar concentration with phyto-derived photosensitization into a synergistic treatment approach.

To evaluate *effective* year-round water disinfection, we assess the suitability of the SEWR approach in addressing the challenge of climate and weather variations and therefore show the relative and realistic performance expectations of a system as impacted by the climate location. SEWR experimental data were combined with computational modeling to evaluate the potential annual performance across three sites within 0–35° latitude. Field testing within realistic application settings demonstrated complete bacterial inactivation at >6 LRV and integration of photosensitizing dyes to

produce >4-log probable virus inactivation. The modeling showed that the integration of multi-treatment mechanisms into the building could provide 61–82 L of purified water per person per square meter daily, year-round, thus meeting the minimum UN daily drinking water requirement of 15 L per person on all sites within the study.

Unlike many incumbent HWTS based on solar disinfection that fail to deliver year-round safe water, with both acute and chronic health and economic impacts, SEWR demonstrates a multi-mechanism approach that could maximize available sunshine to shorten solar water disinfection treatment times in climates with fluctuating solar resources. Field results show that SOPAS temperatures sufficient for complete viral and bacterial inactivation were reached within 28 min at steady state, and a probable >4-log viral inactivation by photosensitization was achieved within 45 min with the Case 4 configuration. Whereas, extrapolated performance with the Case 3 configuration would achieve the same in less than 10 min—meeting EPA requirements and dramatically reducing treatment times compared to conventional SODIS, which typically requires up to 30 h.

Addressing *resource security*, we evaluate the disinfection capacity using modeled system performance to estimate whether the system produces adequate daily water treatment volumes over a typical year to mitigate oversights or added burdens on households. The SEWR approach was demonstrated to provide comprehensive disinfection that guarantees >50 L-pp-m<sup>2</sup> for over two-thirds of the year, namely for 80% of daily yearly demands in Phoenix and 61% for Sololá and Cape Town. The SEWR system could incorporate a building-integrated prefiltration stage, which could boost water production rates to provide annual daily potable water demands of 50 L-pp-m<sup>2</sup> for most of the year in each climate location; fulfilling up to 83% of daily yearly needs in Sololá, 91% in Phoenix, and 73% in Cape Town.

In evaluating the viral inactivation capacity of the SEWR system, in this study, erythrosine-B has numerous benefits as a preliminary model edible photosensitizer, especially for the disinfection of viruses that prove difficult to remove from pretreatment processes<sup>50</sup>. However, we recognize that inconsistent access in countries that do not utilize erythrosine-B in their food systems would create a potential barrier to use in the SEWR system. In the deployment of the SEWR system, we envision using natural photosensitizing compounds that are easily extracted from plants for disinfection, including hypericin extracted from Saint John's Wort and chlorophyll that is extractable from numerous plant sources<sup>51</sup> creating a sustainable and locally accessible disinfection system. Most natural photosensitizers, like many phytochemicals, are hydrophobic and thus require dispersing agents to enable <sup>1</sup>O<sub>2</sub> production in aqueous systems to prevent self-quenching via aggregation. Thankfully, such dispersing agents (e.g., saponins) are abundant in various plants, including agricultural crops such as chickpeas and quinoa, and can be easily extracted<sup>51</sup>. Toward sustainable application in the SEWR system, natural photosensitizers and dispersing agents would be sourced from agricultural byproducts (e.g., chlorophyll extracted from the leaves of residual biomass, saponins extracted from quinoa husks), utilizing resources within agricultural waste streams to improve drinking water disinfection.

Comparing the disinfection kinetics attributed to photosensitization, 10 μM erythrosine-B (i.e., the modeled photosensitizer in this study) has a Chick's Law disinfection rate 10-times that of the 100 μM chlorophyll-saponin system reported in the literature<sup>50,51</sup>. However, when using an edible synthetic dispersant (i.e., 100 μM chlorophyll-sodium dodecyl sulfate (SDS)), the disinfection kinetics for the chlorophyll-SDS system were 17% faster compared to the 10 μM erythrosine-B system<sup>50,51</sup>, showing promise that a natural photosensitizer can suitably enhance virus disinfection rates in the SEWR system. Further, this confirms that 10 μM erythrosine-B models what can be expected when utilizing naturally sourced alternatives. While the exploration of natural photosensitizers and dispersants is a growing field, further investigations into the phytochemicals produced by native flora have the potential to expand the library of natural and sustainably sourced photosensitizers and dispersing agents as input materials into the SEWR system across various geographic application regions. Furthermore, while the photosensitizers mentioned in this work are either edible or

naturally occurring, questions remain regarding impacts on human health, thus, toxicological investigations of the photosensitizers and their photo-bleaching products need to be completed prior to utilization. Likewise, assessment of user acceptability of edible photosensitizing dyes (e.g., riboflavin, hypericin, curcumin, chlorophyll), will be considered in future investigations that consider specific photosensitizers that are compatible with the context within pilot-scale deployment studies.

SEWR presents a building-integrated approach to making solar-based disinfection systems viable and *scalable* for housing, combining multiple functional uses of solar energy for households needs such as energy and heating. The modeled results suggest that SEWR could provide household energy security by delivering daily domestic water heating demands for up to 94% of the year in Phoenix, 88% in Sololá, and 84% of this period in Cape Town. As a result, Cape Town households' energy costs could be halved with the SEWR system relative to the proportional water heating contribution to average household energy bills. Likewise, Phoenix households could benefit from a reduction of up to a fifth of their energy bills using the freely available solar energy of the local climate.

Future work will also include comprehensive technoeconomic assessments of the system affordability, including modeling of household energy and material costs at each deployment site. As a multifunctional building system that leverages building-integrated design to reduce marginal per-function cost, the SEWR system could replace several building systems, including household water disinfection hardware, a portion of the building roofing or glazing, and domestic water heating appliances such as boilers or solar thermal collectors. Accordingly, a complete cost analysis must account for the avoided cost of these standalone systems, rather than treating SEWR as an additive capital expense. In our initial estimates, the primary expense of the SEWR embodiment combines the cost of a roofing assembly with the flow-through water management elements typically associated with solar thermal collectors (e.g., pumps, storage, plumbing). A comparison of material costs suggests that the SEWR system relies on components that are generally less expensive than those used in conventional solar-thermal and CPC-based SODIS collectors, such as avoiding the use of copper tubing, metal reflector components, or insulated glazing. Photosensitizing dyes derived from locally grown plant sources represent negligible material cost relative to commercial catalysts; alternatively, the proxy of edible dye used in this study, erythrosine, has been estimated at US \$0.001–0.002 per liter<sup>50</sup>. Future studies on the system will also assess component durability, dye stability, and year-round performance to refine system sizing and operational feasibility. Future studies on the impact and applications will study the role of distributed HWTS approaches, such as the SEWR system, on drought resilience within various building and urban typologies.

In summation, current solar-driven household water treatment systems cannot guarantee safe water throughout the year in variable solar climates typical of regions below ±35° latitude, across rainy and dry seasons. Here, the SEWR system concept offers a scalable approach that could deliver year-round water safety by synergistically integrating multiple disinfection techniques that on their own cannot guarantee year-round water safety: optical solar concentration is combined with plant-based photosensitizing dyes to disinfect water, while dramatically reducing household energy costs by lowering cooling loads through the redirection of solar heat gain into domestic hot water provision using renewable energy.

## Methods

### System description

The Solar Enclosure for Water Reuse (SEWR) is a building-integrated approach to distributed safe drinking water through accessible renewable energy<sup>36</sup>. This approach could address critical efficacy and adoption limitations of HWTS by demonstrating how simple modifications to existing building envelope designs, incorporating hybrid reactor conditions and multiple solar treatment techniques, can provide adequate water disinfection using available renewable and plant-based resources. The embodiment of SEWR investigated in this study aims to be incorporated into the fenestration and roofing of housing assemblies, ensuring adequate year-

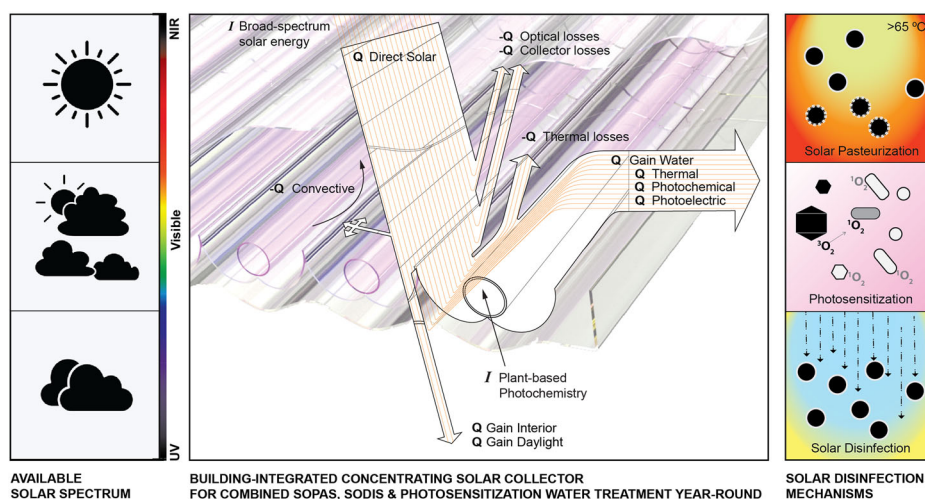


**Fig. 6** | A multifunctional building-integrated solar water treatment concept: A building-integrated concentrating solar-water collection system that provides combined SOPAS, SODIS, and photosensitization to ensure adequate drinking

water disinfection year-round, while providing daylighting and building thermal regulation (Pretorius & Dyson, 2024).

round drinking water disinfection at a minimal additional cost, with ancillary benefits in building thermal regulation and domestic hot water supply (Fig. 6)<sup>35</sup>.

SEWR adopts principles in optical solar concentration, incorporating the geometry of compound parabolic collectors (CPCs) within an insulated building assembly that captures sunlight for water disinfection, water heating, and daylighting, while mediating the heat gain and loss effects across the building envelope. Solar energy incident on the collector aperture is transmitted through an enclosing surface and concentrated onto a quartz glass receiver tube at the optical focal point of a compound parabolic collector (CPC) geometry.

The approach demonstrates an innovative multi-mechanism system integration that hybridizes photoreactor requirements for SOPAS, SODIS, and visible-spectrum photosensitization to maximize the use of available solar energy for disinfection and domestic water heating (Fig. 6). SEWR incorporates photosensitizing dyes that could be sourced inexpensively from locally grown agricultural plants and are highly effective against viruses that many POU approaches fail to remove. To overcome the limited virucidal rate of conventional SODIS, the system demonstrates the application of photosensitization, which generates singlet oxygen (<sup>1</sup>O<sub>2</sub>), an ROS, under visible-spectrum solar irradiation to inactivate >99.99% of water-borne viruses using broad-spectrum sunlight within 10–20 min, in comparison to the incumbent which requires >30 h<sup>50,51</sup>.

With SEWR, we aim to address the interdependence between household resource security factors, such as energy and materials access, that affect the viability of on-site water treatment, while capturing incident solar energy that would otherwise drive up building cooling loads. SEWR adopts established principles of CPC collectors in a roofing-integrated system to capture incident solar energy that is conventionally *either* reflected and wasted *or* absorbed as unwanted heat gain, which is utilized here for multifunctional water disinfection and domestic hot water (DHW) requirements. The building-integrated system has been developed for use in direct solar climates within the 0°–35° latitude range (>5 kWh/day-average) in which daily household needs could be met year-round using renewable bioclimatic resources. SEWR’s multifunctional approach reduces the overall cost of the household systems by providing energy and DHW while lowering household energy demands by providing cool, diffuse daylighting and a comfortable interior through the reactor assembly<sup>35</sup>.

### Reactor description

For field testing, the reactor is constructed to represent a longitudinal flow path through the roofing-integrated collector, flowing upwards in an

inclined orientation that assumes the slope of a roof. Harnessing buoyancy and controlling for air bubble formation with a vertical flow direction, the influent point is at the bottom end of the inclined reactor, and the effluent is at the top.

Representing a portion of a roof assembly, the enclosed CPC geometry is formed between an exterior enclosure surface and an interior-facing pane that insulates the system from the building interior. The reactor first surface enclosure was vacuum-formed in transparent polyethylene terephthalate glycol (PETG) thermoplastic (0.06” thickness), adopting the curvature of a segment of clear corrugated roofing. The CPC reflector geometry was fabricated in vacuum-formed clear PETG (0.03” thickness) to which an adhesive-backed aluminum film (0.2 mm) was applied on the reflector’s first surface.

The reactor is framed in clear cast polymethyl methacrylate (PMMA). The receiver comprises of a quartz glass tube (19 mm ID, 22 mm OD; 90%T, 1.46 refractive index) located at the optical focus point of the CPC reflector and held in alignment by reactor framing members. The receiver is thermally insulated from the reactor frame with rubber grommets at all contact points. To control incident solar irradiation and ambient heating effects, the reactor was clad in a milled polystyrene casing that framed the reactor aperture area facing the sky and an interior aperture area facing the building interior.

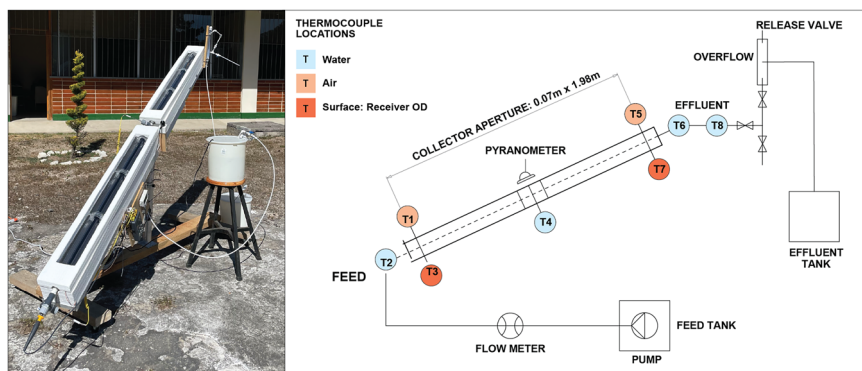
The quartz glass receiver was modified to combine direct irradiation of the water volume with enhanced capacity for thermal conversion of incident solar required for combined SODIS, photosensitization and SOPAS irradiation through the application of a solar absorption coating (SOLKOTE HI/SORB II, SOLEC) oriented towards the optical concentrating reflector geometry (Fig. 4: *Case 2 and Case 4*). Water entering the fluid flow path is irradiated through the tube top surface over the collector aperture area over a particular residence time. Direct irradiation into the water volume through the transparent portion of the receiver enables both SODIS and photosensitization. CPC-reflected energy is absorbed by the solar absorber coating applied to the bottom portion of the glass receiver and transferred into the water for SOPAS heating.

The irradiated collector aperture is 0.070 m by 1.980 m. Within the reactor, an irradiated fluid volume of 0.566 L is channeled through a quartz glass tube with an internal diameter of 0.019 m and a wall thickness of 0.0015 m along a 2 m flow path (1.998 m).

### Reactor configurations

The system can embody several reactor configurations with respect to the relevant water disinfection mechanism, (Fig. 4), either prioritizing optical

**Fig. 7** | Experimental setup of flow-through outdoor reactor testing in Sololá, Guatemala described by a photo of the setup and an accompanying experimental diagram. As shown in the color-coded diagram, time series data included thermocouple measurements of air, water, and surface temperatures within the system at the locations T1-T8, as well as solar irradiance, ambient temperature, and relative humidity measurements. The system was setup as a single flow-through condition with separate feed and effluent tanks.



concentration for direct irradiation of the water volume for SODIS (*Case 1*) or the addition of photosensitizing dyes for photosensitization and SODIS (*Case 3*) or a combination of direct irradiation and indirect irradiation of a thermally absorptive section of the reactor receiver that incorporates capacity for SOPAS heating. With the latter, we considered the performance of SOPAS and SODIS (*Case 2*) and as a synergistic combination of SOPAS, SODIS and photosensitization (*Case 4*).

Field testing in Sololá, Guatemala, used the system configurations of *Case 2* and *Case 4* (Fig. 4) to assess the dominant disinfection mechanisms, SOPAS and photosensitization, for bacterial and viral inactivation, respectively.

For experimental purposes, the photosensitizer selected to demonstrate the disinfection capacity of the SEWR system was erythrosine-B (FD&C Red 3 in the USA), an edible food dye photosensitizer that can remain in the treated water post-solar treatment. Erythrosine-B has well-defined light-dose-dependent disinfection kinetics against the model virus MS2 and *E. coli*, allowing modeling of the SEWR water production rates under various configurations<sup>50,52,53</sup>. Furthermore, erythrosine-B possesses dual functionality in water disinfection, as the virus disinfection kinetics are well-correlated with the fading of the dye's pink color (i.e., photobleaching rate)<sup>50</sup>, providing a unique visual indicator to the user of the SEWR system that the water has been sufficiently treated.

Computational modeling of the disinfection capacity of each mechanism factored in the optimal system configuration for each mechanism and used one of two reactor configurations: a clear receiver for direct irradiation or the half-coated receiver condition for combined irradiation and conversion to heat, as shown in Fig. 4. Modeling compared reactions under direct irradiation (1. SODIS; 3. Photosensitization + SODIS) in a clear receiver or treatment based on thermal conversions (2. SOPAS + SODIS; 4. Combined) in the partially coated receiver configuration. The test reactor was fabricated in a commonly available material, clear Polyethylene terephthalate glycol (PETG), which, like poly(ethylene terephthalate) (PET) bottles used with SODIS, blocks a large portion of UV-B and thereby provides a realistic comparison of the impact of SODIS with the other treatment mechanisms in the field. The modeled disinfection capacity (*Case 1*) assumes ideal reactor materials with 100% transmittance for UV-A and UV-B, which could be achieved using UV-transparent plastics.

### Outdoor field testing

All outdoor system testing under full sun and laboratory analysis were conducted from March–April 2023 on the Universidad del Valle de Guatemala Highlands Campus (Campus Altiplano) in Sololá, Guatemala. Repeat microbial experiments were performed on sunny days with an average insolation of 1064 W/m<sup>2</sup>, with additional experiments conducted in non-ideal cloudy conditions as a low-sun benchmark. Similarly, proxy testing of viral inactivation via measured photosensitizer decay rates was conducted under full sun (~1000 W/m<sup>2</sup>). Due to the complexity of the multiple coupled heat transfer modes (i.e., incoming and reflected solar irradiation, convection inside the

collector tube, convection outside the experimental apparatus, etc.) that govern SOPAS and domestic water heating rates (Fig. 6), outdoor testing under realistic conditions was essential for validating the model and multi-treatment mechanism approach.

All experiments were conducted between 9 am and 1 pm (average 150 min per run). The peak solar hours of the UVG Highlands Campus field site fall within the morning to noon period, after which cloud cover develops due to weather patterns of a high-altitude mountain range.

The reactor was tilted to simulate an inclined roof surface, representing the solar collector integration as a roof light system (Fig. 7). Although the annual average optimal tilt angle (OPTA) for solar applications in Sololá, Guatemala, is 19° (Solargis, 2024), the reactor was oriented at a 25° incline to ensure an average direct normal irradiation of the collector for the experimental period at the field location (April 2023) for experimental purposes. Future studies conducting long-term experimentation will use a fixed incline that is mutually determined by the OPTA for solar systems and building integration constraints (e.g., minimum roof incline of >10° for rainwater shedding).

### Flow control

The proposed system manages optimum solar exposure by adjusting flow rate to match the available insolation, retaining the water volume in the reactor for more extended periods during cloudy conditions or increasing output during peak solar periods when the water is treated more rapidly. As a flow-through system integrated into building roofing, water is treated in a single pass, and untreated water is safely separated from treated water.

The experimentation compared the system's disinfection performance at set effluent temperatures attained with static batch heating and assessed the disinfection capacity in a flow-through condition to evaluate performance consistency. A low-flow submersible pump (KEDSUM, 450 L/h, 8 W) located in the feed tank enabled testing of slow volumetric flow rates of between 10–150 mL/min (1.63E-04–2.45E-03 kg/s) gauged by a flow meter (BROOKS 2520A4L56SVVT) before reticulation into the reactor feed point.

A valve control at the effluent point acted as a safety valve to prevent contamination of treated water by untreated water and to retain heat in the collector volume during static no-flow experimentation. The control valve was opened at each sample point for static, fixed-temperature sampling and was kept open for flow-through experimentation.

Flow-through testing was conducted at 10 mL/min, targeting an effluent temperature >65 °C. Flow-through samples were collected with continuous flow. Feed and effluent tanks in 20 L capped vessels (opaque white, polypropylene) mitigated solar exposure or excess heating above the ambient temperature. A feed tank volume of 6 L was prepared for each experiment.

### Time-series data logging

Thermocouples measured air, water, and surface temperatures within the system at designated points along the flow path length, as described in Fig. 7.

Probes measured the water temperature at the reactor feed and effluent points, at the midline point between the two 1-meter reactor segments, and at an additional effluent temperature control located at the valve (K-type calibrated immersion probe, OMEGA KTSS-HH). The air temperature of the collector cavity was measured at the feed and effluent points at either end of the irradiated flow path length (K-type calibrated bead probe, OMEGA 5LRTC-GG-K-20-36). Likewise, surface temperatures of the glass tube receiver were taken at non-irradiated portions of the tube at the feed and effluent points to measure glass outer diameter (OD) temperatures relative to the ambient air temperature and resulting from heat transfer between the water volume across the glass thickness (K-type calibrated bead probe, OMEGA 5LRTC-GG-K-20-36).

The initial reactor setup involved calibration and quality control checks of probe installations and the longitudinal thermal distribution along the path length. Time-series thermal data was continually logged at 10-s intervals (Onset HOBO UX120-006M). Solar irradiance was also measured at 10-s intervals (Pace Scientific SRS-200/Apogee SP-212-SS silicon-cell pyranometer; 360–1120 nm) with the pyranometer mounted in alignment with the collector aperture plane (maximum deviation of 1°) without shading the collector aperture area and thermally insulated from the support rig to reduce temperature-dependent errors.

Experimental weather data collection included ambient air temperature (Onset HOBO TMC6-HD) and relative humidity (Pace Scientific TRH-100-10FT), with continual time-series data logging (Onset HOBO UX120-006M). Weather data from UVG Campus Altiplano was also sourced through the Meteomatics Weather API.

### Sample collection

The pump, feed, and effluent tanks were disinfected with 95% alcohol between experiments, then rinsed with sterilized deionized (DI) water and left to air-dry. The flow-through system, comprising the flow path between the feed and effluent tanks, as shown in Fig. 7, was flushed with DI water before and after each experiment. All fluid was discharged entirely from the system for overnight storage between experimental days.

Having set up the reactor under full sun in a stationary position, an initial feed supply of 150 mL/min filled the system within 4 minutes. Before starting the experimental run, 300 mL was discharged to flush the system and to draw off heat, stabilizing system temperatures to the ambient conditions. During experimentation in the static batch heating mode, samples (300 mL) were collected at stepped temperature points to compare fluid temperature with bacterial inactivation through SOPAS. Samples were collected at targeted temperature points, including the ambient sample at the run start (0 min), and increased mid-point fluid temperatures of 35 °C, 50 °C, and 65 °C. A repeat sample at 65 °C verified the bacterial disinfection capacity and residence time with consecutive batch heating. At each temperature point, samples were collected from the fluid volume in the top half of the reactor's irradiated water volume. Each sample represented the temperature distribution between the midpoint and effluent. Static batch heating samples were collected at 100 mL/min flow rate and discharged within 3 min.

Following the static batch heating sampling, the reactor simulated flow-through conditions at 10 mL/min to assess microbial inactivation at steady-state. Once the temperature differential between the feed and effluent points of the flow-through condition stabilized, a 300 mL sample was collected continuously from the out-flow point at a 10–15 mL/min flow rate (20 min sample period).

Each 300 mL sample was collected in autoclaved Pyrex bottles and stored in the dark before analysis (triplicate testing, 100 mL). No sampling was collected from the effluent tank; it was only done directly at the reactor effluent point. Dark control samples of feed water used in the feed tank were collected and stored indoors for all experiments/repeats.

*E. coli* inactivation testing using the *Case 2* configuration was conducted on consecutive days from 11 to 13 April 2023. As part of the experimental design, we conducted static and flow-through testing in series to simulate dynamic flow control once the system had reached a steady state. Experiments based on the static batch and flow-through test protocols were

conducted daily, in series, over the consecutive days of April 11, 12, and 13, 2023. At each sampling point, three samples of 100 mL each were tested in triplicate per the bacterial enumeration protocols. The dye photobleaching experiments using the *Case 4* configuration were conducted on March 23, 2023, at a concentration of 10 µM erythrosine-B. Replicate absorbance measurements at 526 nm were taken per sample. Long-term outdoor testing of thermal performance was conducted on non-consecutive days from February 27 to March 7, 2023.

### Test water preparation

The water supply for the Universidad del Valle de Guatemala (UVG) Campus Altiplano in Sololá is sourced from a private well located on campus. The water extracted is lightly chlorinated and pumped into an elevated tank for storage and distribution across the entire campus. Since 2022, management has conducted biannual water quality assessments on a routine basis. Samples were collected on January 16, 2023, from the well, storage tank, and one tap outlet to assess the water's characteristics. The test water, sourced from the tap, complies with the standards for drinking water established by the U.S. Environmental Protection Agency (EPA), as outlined in Table S2 (Supplementary Information).

Dechlorination procedure: water was collected from the tap into an acid-washed bucket. The container was cleaned with 0.1 N hydrochloric acid and subsequently rinsed three times with distilled water. We added 0.3 mL sodium thiosulfate (25 ppt) to the tap water and left it to stand for 1 h before the addition of *Escherichia coli* (*E. coli*).

### Bacterial inactivation/*E. coli* enumeration

Bacterial enumeration, which demonstrates the system's SOPAS disinfection capacity, was assessed as a measure of the log reduction of colony-forming units (CFU) through the bacterial enumeration of water samples within several temperature ranges. To evaluate the maximum Log Reduction Value (LRV), the system was challenge-tested with feedstock solutions at a 10<sup>5</sup>–10<sup>6</sup> CFU/mL *E. coli* concentration (based on enumerated dark control) and repeat tested under full sun in warm ambient conditions (clear sky, >1100 W/m<sup>2</sup>, 23 °C, 59% RH ambient) on consecutive days from 11 to 13 April 2023.

The *E. coli* strain (C-3000) was obtained from the American Type Culture Collection (ATCC). Freeze-dried pellets were revived per the ATCC guidelines and grown in fresh liquid medium (Tryptone Soya Broth, Millipore 22092-500 G), incubated at 37 °C until the culture reached the stationary phase, as determined by optical density measurements. Bacterial culture growth was suspended for refrigerator storage by inoculating agar slabs and suspended in phosphate-buffered saline (PBS, 1.0 mM, pH 7.2) for storage at 2–4 °C.

Before experimentation, saturated *E. coli* stock solution was grown overnight in broth medium under incubation to reach a 10<sup>9</sup> CFU/mL concentration. The saturated *E. coli* solution was diluted into dechlorinated tap water at a target initial concentration of 10<sup>9</sup> CFU/mL. Dechlorinated tap water was sourced from the Universidad del Valle de Guatemala campus in Sololá, Guatemala, and was deemed representative of untreated household source water. *E. coli* enumeration used the membrane-filtration (MF) method<sup>54</sup> in selective media (m-FC Agar, OXOID MM747) and counted after 24 hr incubation at 37 °C.

Samples collected at several temperature-time conditions were evaluated by drinking water standards with the expectation of lower microbial concentrations. With triplicate testing of each 300 mL sample, 100 mL samples were suction-filtered through 0.45 µm membranes (Millipore HAWG047S) and triplicate plated on selective medium agar plates. Dark control and feedstock solutions at higher probable *E. coli* concentrations were membrane filtered and plated in 10 mL, 1 mL, and 0.1 mL volumes.

### Indirect assessment of viral inactivation based on dye photobleaching experiment

In the present study, virus inactivation was assessed indirectly through the strong kinetic correlation between photobleaching (i.e., color loss) and virus

LRV with erythrosine-B—a photosensitizing dye. Direct viral viability assessment was not feasible due to field research constraints, as the MS2 bacteriophage stock was non-viable upon arrival in Sololá and could not be revived or replaced. Erythrosine-B previously demonstrated kinetic relationships between  $^1\text{O}_2$  production, extent of photobleaching, and MS2 bacteriophage inactivation under comparable light conditions (i.e., 1000 W/m<sup>2</sup> via solar simulator) to those experienced during field testing of the SEWR system in Sololá<sup>50</sup>. Particularly, under these sunlight conditions, photobleaching exhibits a linear relationship with the steady-state concentration of  $^1\text{O}_2$  over a range of approximately 10–70% loss. Our field measurements largely fell within this linear regime, indicating that applying the established correlation between photobleaching and  $^1\text{O}_2$  production to our dataset requires minimal extrapolation. Together with the CT relationship between MS2 bacteriophage and  $^1\text{O}_2$ <sup>50</sup>, this correlation provides an appropriate basis to indirectly assess the potential MS2 bacteriophage disinfection capacity of the SEWR system by observing photobleaching color loss during field testing.

Outdoor testing of the SEWR system was conducted in flow-through conditions (10 mL/min), using DI water spiked with 10  $\mu\text{M}$  erythrosine-B. Five milliliters aliquots were taken at timestamped sample points (0, 15, 30, 45, 60, 75, 90 min) and immediately stored under dark conditions before analysis. Photobleaching was quantified by the loss of absorbance at the absorption maximum of erythrosine-B (526 nm) using UV–vis spectroscopy (Merck spectrophotometer Spectroquant Pharo 300).

### Disinfection capacity modeling

Disinfection capacity is defined as the amount of disinfected water per unit surface area (i.e., the area of roofing allocated to the building-integrated solar collector) and unit time scale. This study calculated the SEWR system disinfection capacity as a function of local time and day in three locations: Sololá, Guatemala; Phoenix, Arizona, USA; and Cape Town, South Africa. The modeling investigated the contribution of each disinfection mechanism (i.e., SODIS, photosensitization, and SOPAS) to the disinfection capacity of the SEWR system, evaluated individually and in combination. Four case types in Fig. 4 were considered: (1) SODIS only (2) SOPAS with SODIS, (3) photosensitization with SODIS, and (4) all the latter in a multi-mechanism system. In pasteurization cases, the partially coated receiver configuration was considered (Cases 2 and 4), whereas a clear receiver was used for direct irradiation cases, SODIS and photosensitization (Fig. 4: Cases 1 and 3).

To investigate the potential system performance if developed to incorporate multi-barrier water treatment, we evaluated the disinfection capacity of the system, with and without a proxy prefiltration stage. For this comparison, the prefiltration stage was assumed to achieve a 4-log reduction for bacteria but no virus removal. Per US EPA and WHO regulations<sup>24,26,55</sup>, 4 LRV for bacteria and viruses was the minimum requirement for the system to claim disinfection. For SOPAS, target effluent temperatures to achieve thermal inactivation (>4 LRV) for bacteria and viruses were 65 and 75 °C, respectively<sup>20,56</sup>.

A detailed procedure to calculate the disinfection capacity is described in Supplementary Information (Text S1–S4), and the R software was used for all modeling work and disinfection capacity prediction. In summary, the modeling considered solar irradiance, ambient temperature, local hour, and local day to predict disinfection capacity for various cases (Fig. 4). The relationship between the optical efficiency and the azimuth/elevation angle in each case (Fig. 4), determined from a ray tracing simulation (Text S5), allowed for predicting optical efficiency as a function of the local hour and day in target cities. By combining real solar irradiance and ambient temperature with optical efficiency simulation, we estimated the disinfection capacity for each case (Fig. 4) across all cities. For SODIS and photosensitization, we calculated the steady-state concentration of ROS using the extinction coefficient and quantum yield, subsequently determining the disinfection capacity by factoring in the residence time. For SOPAS, the collector efficiency was used to calculate the exit water temperature, and the required residence time to reach 65 °C or 75 °C was determined to assess disinfection capacity. The

collector efficiency was determined per methods standards for concentrating collectors<sup>57–59</sup>, described in Supplementary Information (Text S7).

### Data availability

Data availability: Data available from the corresponding author upon reasonable request.

### Code availability

The R software and the freely available R packages were used for all data exploration. The codes that support the findings of this study are available from the corresponding author upon reasonable request.

Received: 17 September 2025; Accepted: 30 November 2025;

Published online: 05 February 2026

### References

- WHO. Drinking-water Factsheet. <https://www.who.int/news-room/fact-sheets/detail/drinking-water> (2023).
- Troeger, C. et al. Estimates of the global, regional, and national morbidity, mortality, and aetiologies of diarrhoea in 195 countries: a systematic analysis for the Global Burden of Disease Study 2016. *Lancet Infect. Dis.* **18**, 1211–1228 (2018).
- Wolf, J. et al. Burden of disease attributable to unsafe drinking water, sanitation, and hygiene in domestic settings: a global analysis for selected adverse health outcomes. *Lancet* **401**, 2060–2071 (2023).
- United Nations. *World Urbanization Prospects: The 2018 Revision*. UN Dept Economic & Social Affairs, Population Division. <https://www.un.org/en/desa/2018-revision-world-urbanization-prospects> (2019).
- Rosa, G. & Clasen, T. Estimating the scope of household water treatment in low- and medium-income countries. *Am. J. Trop. Med. Hyg.* **82**, 289–300 (2010).
- Javidi, A. & Pierce, G. U. S. Households' perception of drinking water as unsafe and its consequences: examining alternative choices to the tap. *Water Resour. Res.* **54**, 6100–6113 (2018).
- Pierce, G. & Gonzalez, S. R. Public drinking water system coverage and its discontents: the prevalence and severity of water access problems in California's mobile home parks. *Environ. Justice* **10**, 168–173 (2017).
- Wu, J., Cao, M., Tong, D., Finkelstein, Z. & Hoek, E. M. V. A critical review of point-of-use drinking water treatment in the United States. *npj Clean. Water* **4**, 1–25 (2021).
- WHO. *Guidelines for Drinking-Water Quality: Fourth Edition, Incorporating the First and Second Addenda* (WHO, 2022).
- Srivastav, A. L., Patel, N. & Chaudhary, V. K. Disinfection by-products in drinking water: Occurrence, toxicity and abatement. *Environ. Pollut.* **267**, 115474 (2020).
- Schmidt, W.-P. & Cairncross, S. Household water treatment in poor populations: is there enough evidence for scaling up now? *Environ. Sci. Technol.* **43**, 986–992 (2009).
- Chaúque, B. J. M. & Rott, M. B. Solar disinfection (SODIS) technologies as alternative for large-scale public drinking water supply: advances and challenges. *Chemosphere* **281**, 130754 (2021).
- WHO. *Results of Round II of the WHO International Scheme to Evaluate Household Water Treatment Technologies* (WHO, 2019).
- CAWST. Household water treatment and safe storage (HWTS) knowledge base: technical information: boiling; Center for Affordable Water and Sanitation Technology. <https://www.hwts.info/products-technologies/819dad5c/boiling/technical-information> (2017).
- Sobsey, M. D. & WHO. *Managing water in the home: accelerated health gains from improved water supply* (WHO, 2002).
- Islam, M. F. & Johnston, R. B. Household pasteurization of drinking-water: the chulli water-treatment system. *J. Health Popul. Nutr.* **24**, 356–362 (2006).

17. Nair, S. S. et al. Life cycle assessment comparison of point-of-use water treatment technologies: Solar water disinfection (SODIS), boiling water, and chlorination. *J. Environ. Chem. Eng.* **11**, 110015 (2023).
18. Andreatta, D. *A summary of water pasteurization techniques* (The solar cooking archive, 1994).
19. Feachem, R. G., Bradley, D. J., Garelick, H. & Mara, D. D. *Sanitation and disease: health aspects of excreta and wastewater management*. <https://www.cabdirect.org/cabdirect/abstract/19852018217> (1983).
20. Spinks, A. T., Dunstan, R. H., Harrison, T., Coombes, P. & Kuczera, G. Thermal inactivation of water-borne pathogenic and indicator bacteria at sub-boiling temperatures. *Water Res.* **40**, 1326–1332 (2006).
21. Jeon, I., Ryberg, E. C., Alvarez, P. J. & Kim, J.-H. Technology assessment of solar disinfection for drinking water treatment. *Nat. Sustain.* **5**, 801–808 (2022).
22. EST. Solar water heating. *Energy Saving Trust* <https://energysavingtrust.org.uk/advice/solar-water-heating/> (2024).
23. WHO. Emergency Treatment of Drinking Water at Point-of-Use. WHO-Technical Notes for Emergencies No. 5. *World Health Organization (WHO): Geneva, Switzerland* (2005).
24. WHO. *Evaluating Household Water Treatment Options Health-Based Targets and Microbiological Performance Specifications*. <https://www.who.int/publications-detail-redirect/9789241548229> (2011).
25. Fisher, M. B., Iriarte, M. & Nelson, K. L. Solar water disinfection (SODIS) of *Escherichia coli*, *Enterococcus* spp., and MS2 coliphage: effects of additives and alternative container materials. *Water Res.* **46**, 1745–1754 (2012).
26. US EPA. *National Primary Drinking Water Regulations: Long Term 2 Enhanced Surface Water Treatment Rule* (Federal Register, 2006).
27. DESA, U. United Nations, Department of Economic and Social Affairs, Population Division. *World Urbanization Prospects: the 2018 Revision* (Online Edition, 2018).
28. Chaúque, B. J. M., Brandão, F. G. & Rott, M. B. Development of solar water disinfection systems for large-scale public supply, state of the art, improvements and paths to the future – A systematic review. *J. Environ. Chem. Eng.* **10**, 107887 (2022).
29. Chaúque, B. J. M. et al. Why do low-cost point-of-use water treatment technologies succeed or fail in combating waterborne diseases in the field? A systematic review. *J. Environ. Chem. Eng.* **11**, 110575 (2023).
30. Vidal, A. & Diaz, A. I. High-performance, low-cost solar collectors for disinfection of contaminated water. *Water Environ. Res.* **72**, 271–276 (2000).
31. Polo-López, M. I. et al. Elimination of water pathogens with solar radiation using an automated sequential batch CPC reactor. *J. Hazard. Mater.* **196**, 16–21 (2011).
32. Ubomba-Jaswa, E., Fernández-Ibáñez, P., Navntoft, C., Polo-López, M. I. & McGuigan, K. G. Investigating the microbial inactivation efficiency of a 25 L batch solar disinfection (SODIS) reactor enhanced with a compound parabolic collector (CPC) for household use. *J. Chem. Technol. Biotechnol.* **85**, 1028–1037 (2010).
33. Martínez-García, A. et al. Assessment of a pilot solar V-trough reactor for solar water disinfection. *Chem. Eng. J.* **399**, 125719 (2020).
34. Gill, L. W. & Price, C. Preliminary observations of a continuous flow solar disinfection system for a rural community in Kenya. *Energy* **35**, 4607–4611 (2010).
35. Pretorius, M. & Dyson, A. *Farming Secure Water: Resituating the Water-Energy-Food Nexus within Recombinant Building Envelopes* (Fabricate, 2024).
36. Dyson, A. et al. Solar enclosure for water reuse. U.S. Patent No. 9090486B2 (2015).
37. McGuigan, K. G. et al. Solar water disinfection (SODIS): a review from bench-top to roof-top. *J. Hazard. Mater.* **235–236**, 29–46 (2012).
38. Mbonimpa, E. G., Vadheim, B. & Blatchley, E. R. Continuous-flow solar UVB disinfection reactor for drinking water. *Water Res.* **46**, 2344–2354 (2012).
39. McLoughlin, O. A., Ibáñez, P. F., Gemjak, W., Rodríguez, S. M. & Gill, L. W. Photocatalytic disinfection of water using low cost compound parabolic collectors. *Sol. Energy* **77**, 625–633 (2004).
40. Luzi, S., Tobler, M., Suter, F. & Meierhofer, R. *SODIS manual: Guidance on solar water disinfection*, 1–18 (SANDEC, Department of Sanitation, Water and Solid Waste for Development, 2016).
41. *The Sphere Handbook: Humanitarian Charter and Minimum Standards in Humanitarian Response* (Sphere Association, 2018).
42. UN. *United Nations (UN) General Assembly Resolution 64/292: The Human Right to Water and Sanitation* (United Nations General Assembly, 2010).
43. US EIA. *U.S. Energy Information Administration - EIA - 2020 Residential Energy Consumption Survey (RECS)*. <https://www.eia.gov/consumption/residential/data/2020/> (2020).
44. CSIR. *Council for Scientific and Industrial Research (CSIR) 2016. Forecasts of Electricity Demand in South Africa (2014–2050) Using the CSIR Sectoral Regression Model*. <http://www.energy.gov.za/IRP/2016/IRP-AnnexureB-Demand-forecasts-report.pdf> (2016).
45. Henry, C. L. et al. How will renewable energy development goals affect energy poverty in Guatemala? *Energy Econ.* **104**, 105665 (2021).
46. INE. *Encuesta Nacional de Condiciones de Vida – ENCOVI 2011* (INE, 2011).
47. Meireles, I., Sousa, V., Bleys, B. & Poncelet, B. Domestic hot water consumption pattern: relation with total water consumption and air temperature. *Renew. Sustain. Energy Rev.* **157**, 112035 (2022).
48. ASHRAE. *ASHRAE Guideline 12-2000—Minimizing the Risk of Legionellosis Associated with Building Water Systems* (ASHRAE, 2000).
49. Gleick, P. H. Basic water requirements for human activities: meeting basic needs. *Water Int.* **21**, 83–92 (1996).
50. Ryberg, E. C., Chu, C. & Kim, J. H. Edible dye-enhanced solar disinfection with safety indication. *Environ. Sci. Technol.* **52**, 13361–13369 (2018). vol.
51. Ryberg, E. C., Knight, J. & Kim, J.-H. Farm-to-tap water treatment: naturally-sourced photosensitizers for enhanced solar disinfection of drinking water. *ACS EST Eng.* **1**, 86–99 (2021).
52. Liu, Y. et al. Enhancement of *E. coli* inactivation by photosensitized erythrosine-based solar disinfection under weakly acidic conditions. *Water Res.* **212**, 118125 (2022).
53. Silva, A. F. Antimicrobial photodynamic inactivation mediated by rose bengal and erythrosine is effective in the control of food-related bacteria in planktonic and biofilm states. *Molecules* **23**, 1–18 (2018).
54. Rice, E. W., Bridgewater, L. & Association, A. P. H. Standard methods for the examination of water and wastewater (American public health association Washington DC, 2012).
55. WHO. *Guidelines for drinking-water quality*, 4th edn (WHO, 2011).
56. Sanciolo, P. et al. *Pasteurisation for production of class A recycled water: a report of a study funded by the Australian Water Recycling Centre of Excellence*. <http://vuir.vu.edu.au/> (2015).
57. Duffie, J. A. & Beckman, W. A. *Solar Engineering of Thermal Processes* (Wiley, 2013).
58. *DIN EN 12975-2:2006 - Thermal solar systems and components - Solar collectors - Part 2: Test methods*; EN 12975, German version EN 12975-2:2006 (2006).
59. Kalogirou, S. A. Solar thermal collectors and applications. *Prog. Energy Combust. Sci.* **30**, 231–295 (2004).

## Acknowledgements

This work was partly supported by the Environmental Protection Agency P3 Student Grant (#SU840165), the NSF Nanosystems Engineering Research Center for Nanotechnology-Enabled Water Treatment (NEWT) (#EEC-1449500) and the Whitney and Betty MacMillan Center for International and Area Studies (International Dissertation Research Fellowship, Yale University).

## Author contributions

M.P.: Conceptualization, Methodology, Investigation, Data curation, Writing—Original Draft, Visualization, Funding acquisition; I.J.: Methodology (creation of model), Investigation, Writing—Original Draft, Visualization, Formal analysis; M.M.M.-F.: Methodology, Investigation, Resources; N.N.: Methodology; J.L.G.: Supervision; E.R.: Writing—Review & Editing; M.M.D.: Methodology, Writing—Review & Editing; J.-H.K.: Methodology, Writing—Review & Editing, Resources, Supervision; A.D.: Conceptualization, Methodology, Resources, Visualization, Writing—Review & Editing, Funding acquisition, Supervision, Anchor Author. All authors read and approved the final manuscript.

## Competing interests

The authors declare that a patent application related to the work reported in this article has been filed. Patent application number: US 63/948,316.

## Additional information

**Supplementary information** The online version contains supplementary material available at <https://doi.org/10.1038/s41545-025-00539-2>.

**Correspondence** and requests for materials should be addressed to Mandi Pretorius or Inhyeong Jeon.

**Reprints and permissions information** is available at <http://www.nature.com/reprints>

**Publisher's note** Springer Nature remains neutral with regard to jurisdictional claims in published maps and institutional affiliations.

**Open Access** This article is licensed under a Creative Commons Attribution-NonCommercial-NoDerivatives 4.0 International License, which permits any non-commercial use, sharing, distribution and reproduction in any medium or format, as long as you give appropriate credit to the original author(s) and the source, provide a link to the Creative Commons licence, and indicate if you modified the licensed material. You do not have permission under this licence to share adapted material derived from this article or parts of it. The images or other third party material in this article are included in the article's Creative Commons licence, unless indicated otherwise in a credit line to the material. If material is not included in the article's Creative Commons licence and your intended use is not permitted by statutory regulation or exceeds the permitted use, you will need to obtain permission directly from the copyright holder. To view a copy of this licence, visit <http://creativecommons.org/licenses/by-nc-nd/4.0/>.

© The Author(s) 2026